SUPPORTING INFORMATION

Application of Naphthalenediimide Derivatives as Self-Assembled Electron Selective Contacts in CdSe@ZnS Quantum Dots LEDs

Maria Méndez,[1] Abarna Sekar,[2] Dylan Wilkinson,[2] Margarita Gracia,[1] Andrea Di Vera,[1] Laia Marín-Moncusí,[1] José G. Sánchez,[1] Fabian Pino,[3] Rafael S. Sánchez,[3] Iván Mora-Seró,[3] Michele Cariello,[2] Emilio Palomares,[1,4] Graeme Cooke,[2*] Eugenia Martínez-Ferrero,[1*]

[1] Institute of Chemical Research of Catalonia-The Barcelona Institute of Science and Technology (ICIQ-BIST), Avda. Països Catalans 16, 43007 Tarragona, Spain.
[2] School of Chemistry, University of Glasgow, Glasgow G12 8QQ, U.K.
[3] Institute of Advanced Materials (INAM), Universitat Jaume I (UJI), Avenida de Vicent Sos Baynat, s/n, 12071 Castelló de la Plana, Castellón, Spain
[4] Catalan Institution for Research and Advanced Studies (ICREA), 08010 Barcelona, Spain
* Correspondence: GC: Graeme.Cooke@glasgow.ac.uk; Tel +44 0141 330 5500; EMF: emartinez@iciq.es, Tel + 34 977920200

EXPERIMENTAL SECTION

Characterization techniques of the molecules in solution

UV-vis **absorption** and **emission** spectra were recorded using Shimadzu UV-3600 and a Shimadzu RF-5301PC, respectively. The spectra were recorded in DMF solutions ($C = 5 \times 10^{-5}$ M). The emission spectrum was recorded with λ_{exc} = 381 nm (maximum of absorption). Both samples have identical optical properties. An optical band gap was calculated from the cut off wavelength ($\lambda_{cut\ off}$).

The **electrochemistry** was performed using a CH-instruments CHI-440A electrochemical workstation. The samples were dissolved in anhydrous dimethyl formamide (DMF) ($C = 5 \times 10^{-4}$ M), and recorded using a Pt disk working electrode, a Pt wire auxiliary electrode and a silver wire pseudo-reference electrode. Tetrabutylammonium hexafluorophosphate (TBAPF$_6$) was used as a supporting electrolyte ($C = 1 \text{ x } 10^{-1}$ M) and the results were referenced to the Fc$^+$/Fc redox potential, with ferrocene used as an external reference. Samples were purged with N$_2$ gas for 2 minutes prior to measurements.

Theoretical calcultions

The compounds were modelled using Gaussian 09 and results were visualised using GaussView [32]. Both molecules were optimized with a B3LYP functional and a 6-311G(d,p) basis set. A frequency calculation was performed to make sure that the molecules are at an energy absolute minimum.

Characterization techniques of the molecules deposited onto ITO

Contact angle measurements were done with an Attention Theta Flex optical tensiometer using sessile water drop analysis.

Atomic Force Microscopy (AFM) measurements were performed in tapping mode on a Molecular Imaging model Pico SPM II (pico+). Images were recorded with silicon probes with a radius of 1 nm and at the resonant frequency of 150 kHz. The root-mean-squares were calculated with the open-source Gwyddion V2.55 software.

X-ray photoelectron spectroscopy (XPS) analysis was performed at SRCiT (URV) using a ProvenX-NAP (Specs Surface Nano Analysis GmbH, Berlin, Germany) spectrometer (totally funded by Ministerio de Ciencia e Innovación and European Union "Next Generation", project EQC2021-007785-P) with a dual (AlKα = 1487 eV/AgLα = 2984 eV) monochromatic X-ray source (μFocus450). The measurements were collected under these conditions: the power of X-ray of 100 W (AlKα anode), the hemispherical analyzer operating in the main fixed analyzer transmission mode, the entrance slit of 7 x 20mm and the exit slit open with mesh. The beam spot size at the sample position was around 200 microns in diameter. The data were recorded with a PHOIBOS 150 NAP 1D-DLD and the total pressure in the main vacuum chamber during analysis was better than 1×10^{-9} mbar. To obtain more detailed information about chemical structure, oxidation states, etc., high-resolution spectra were recorded from individual peaks at 30 eV pass energy and 0.3 eV step size. Flood gun source had to be used in order to compensate the charge due to the insulating properties of the samples. Each specimen was analyzed at an emission angle of 0° as measured from the surface normal. Assuming typical values for the electron attenuation length of relevant photoelectrons, the XPS analysis depth ranges between 5 and 10 nm for a flat surface. Data processing was performed using CasaXPS processing software version 2.3.26.PR1.0 (Casa Software Ltd., Teignmouth, UK). The atomic concentrations of the detected elements were calculated using integral peak intensities and the sensitivity supplied by the manufacturer. Binding energies were referenced to the C1s peak at 284.8 eV (adventitious carbon).

The **electron mobility** (μ_e) was determined by the space-charge limited current (SCLC) method in electron-only devices with the structure ITO/SAMs/QD/TPBi/Ag. The J-V curves were recorded under dark conditions by a Keithley source measurement unit (model 2400) in a forward range.

The J-V curve can be modelled using the Mott-Gurney equation (Equation (S1)):

$$J = \frac{9}{8}\varepsilon\varepsilon_0\mu\frac{V^2}{L^2}e^{\left(0.89\beta\sqrt{\frac{V}{L}}\right)} \qquad \text{(S1)}$$

where ϵ is the relative permittivity of the material, ϵ_0 is the permittivity of free space (8.854×10^{-8} F/cm), μ is the electron mobility (cm²/V·s), V is the applied bias (in V), L is the thickness of the QDs (50 nm) and β is the Poole-Frenkel factor.

Steady-state photoluminescence (PL) was recorded using a Spectrofluorimeter Fluorolog from Horiba Jobin Yvon Ltd. with PMT and InGaAs detectors. **Time-correlated single photon counting (TCSPC)** measurements were done on the instrument Edinburgh Instruments LifeSpec-II with an excitation source of 405 nm. The decays were fitted to a biexponential equation (Equation (S2)):

$$\tau(t) = A_1 e^{-\left(\frac{t}{\tau 1}\right)} + A_2 e^{-\left(\frac{t}{\tau 2}\right)} \qquad \text{(S2)}$$

where A1 and A2 are the amplitude of the radiative decay lifetime and τ represent the lifetime values. The estimation of the average lifetime was estimated according to Equation (S3):

$$\tau_{average} = \sum \alpha_i \tau_i ; \text{where } \alpha_i = \frac{A_i \tau_i}{\sum A_i \tau_i} \qquad \text{(S3)}$$

Characterization of the devices

The variations of the luminance and the current density as a function of the applied bias for the n-i-p LEDs were recorded using a Konica Minolta IS 100 camera and a Keithley 2400 Unit as voltage/current source, respectively. The performance of the p-i-n LEDs and the characteristics of the emitted light were measured with an external quantum efficiency (EQE) measurement system (Hamamatsu C9920-12).

SUPPLEMENTARY FIGURES AND TABLES

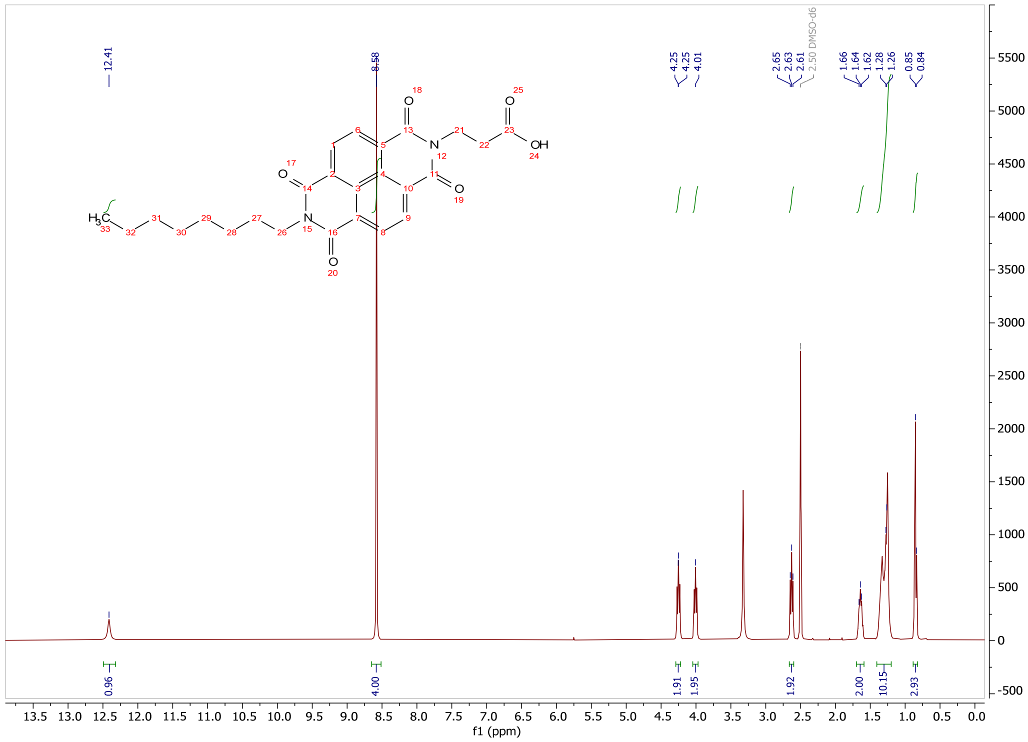

Figure S1. ^{1}H NMR of **SAM3** in *d6*-DMSO.

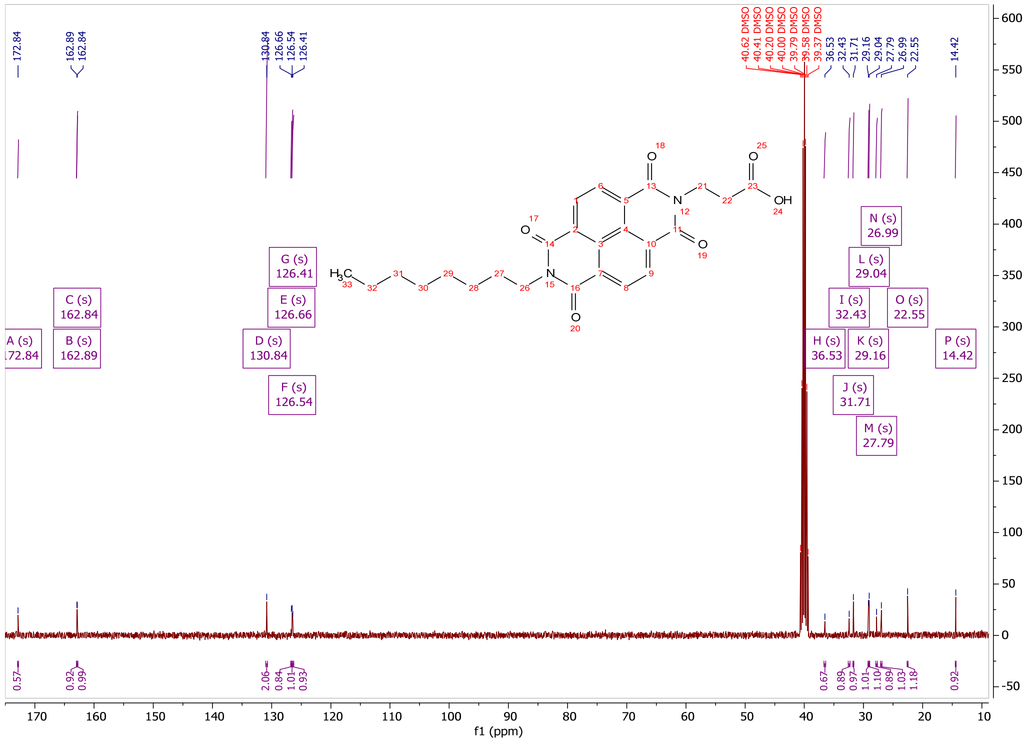

Figure S2. ^{13}C NMR of **SAM3** in *d6*-DMSO.

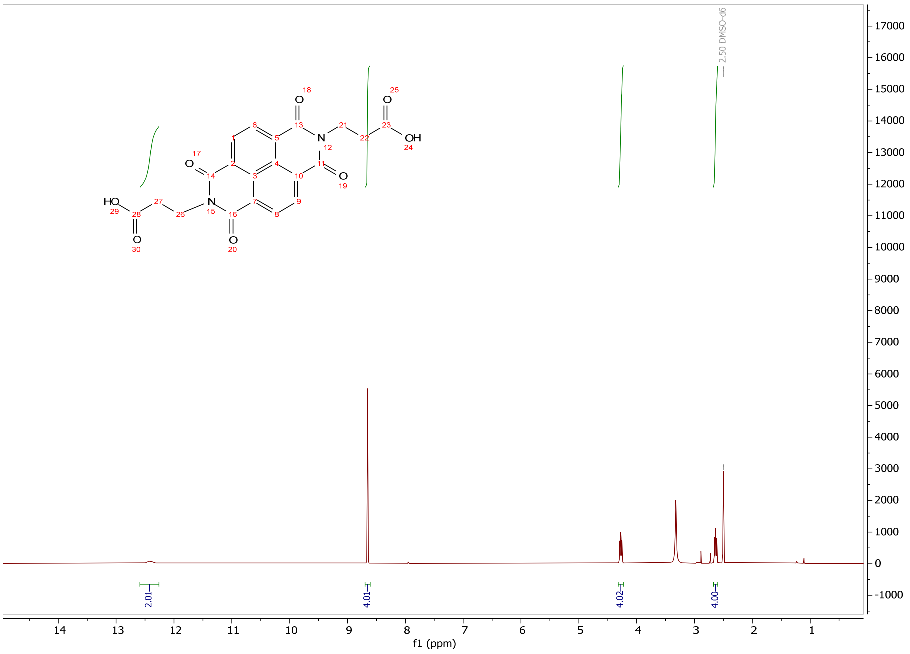

Figure S3. ^{1}H NMR of **SAM12** in *d6*-DMSO.

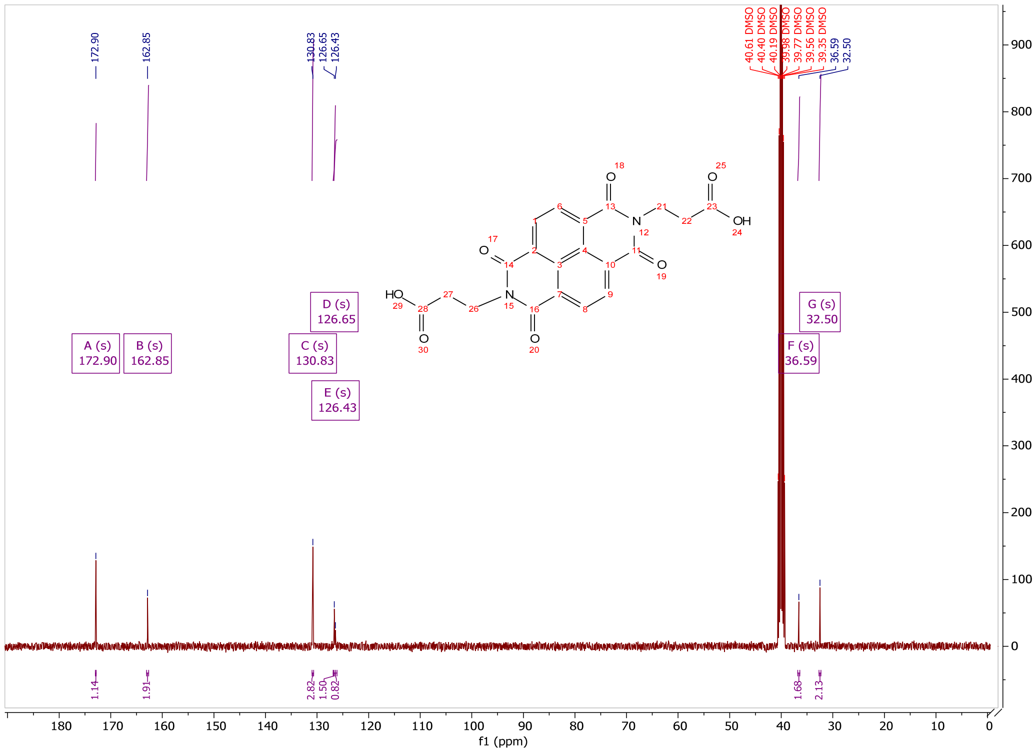

Figure S4. ^{13}C NMR of **SAM12** in *d6*-DMSO.

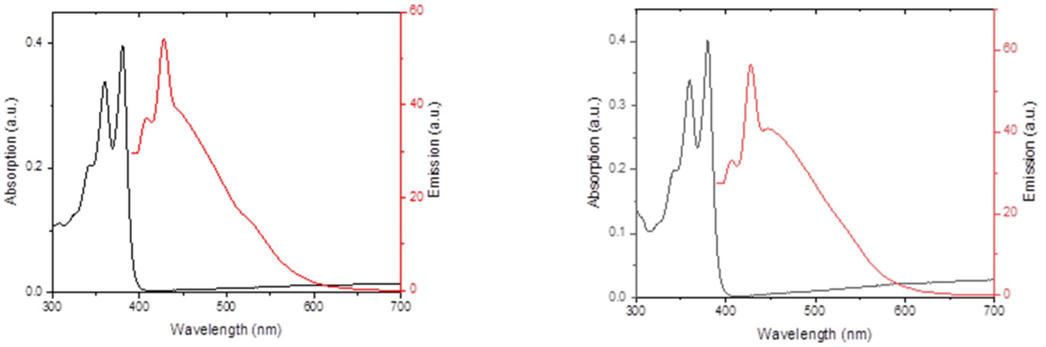

a b

Figure S5. UV-vis (black) and fluorescence (red) spectra of (a) **SAM3** and (b) **SAM12** in DMF solution (C = 5 × 10^{-5} M).The excitation wavelength for the fluorescence measurements was fixed at 381 nm.

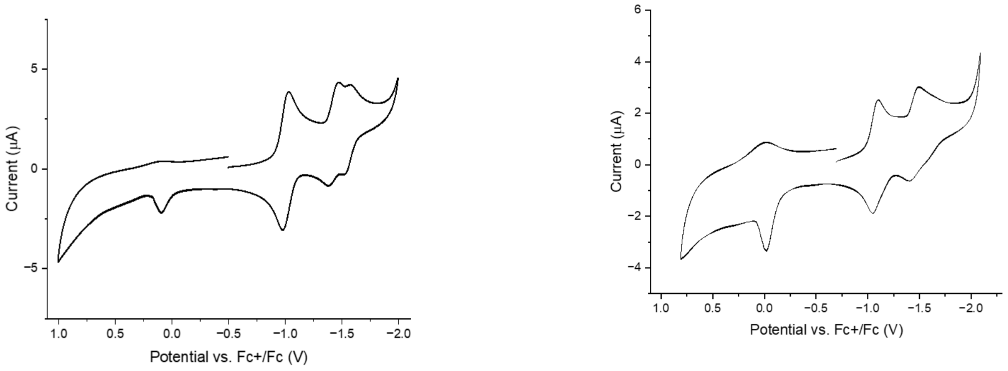

a b

Figure S6. Cyclic voltammetry of (a) **SAM3** and (b) **SAM12** measured in anhydrous DMF (C = 5 × 10^{-4} M), using a Pt disk working electrode, a Pt curly wire auxiliary electrode and a silver wire pseudo-reference electrode. $TBAPF_6$ was used as a supporting electrolyte (C = 0.1 M) and the results were referenced to the Fc^+/Fc redox potential.

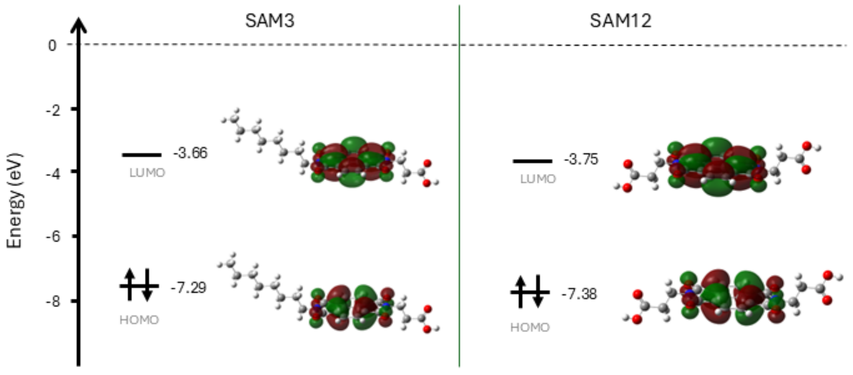

Figure S7. HOMO and LUMO of **SAM3** and **SAM12** estimated by DFT calculations.

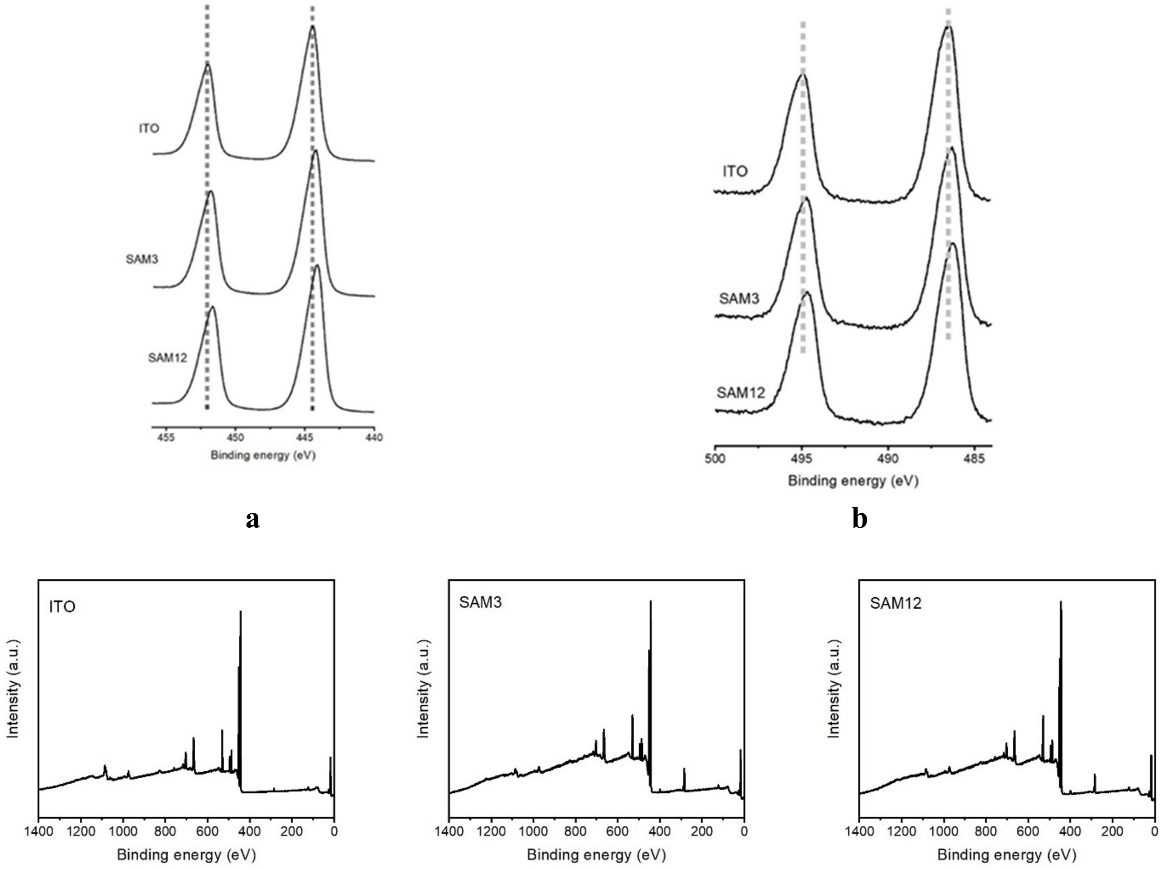

a **b**

c **d** **e**

Figure S8. XPS high-resolution spectra of (a) In 3d and (b) Sn 3d and survey spectra of (c) ITO, (d) ITO/**SAM3** and (e) ITO/**SAM12** films.

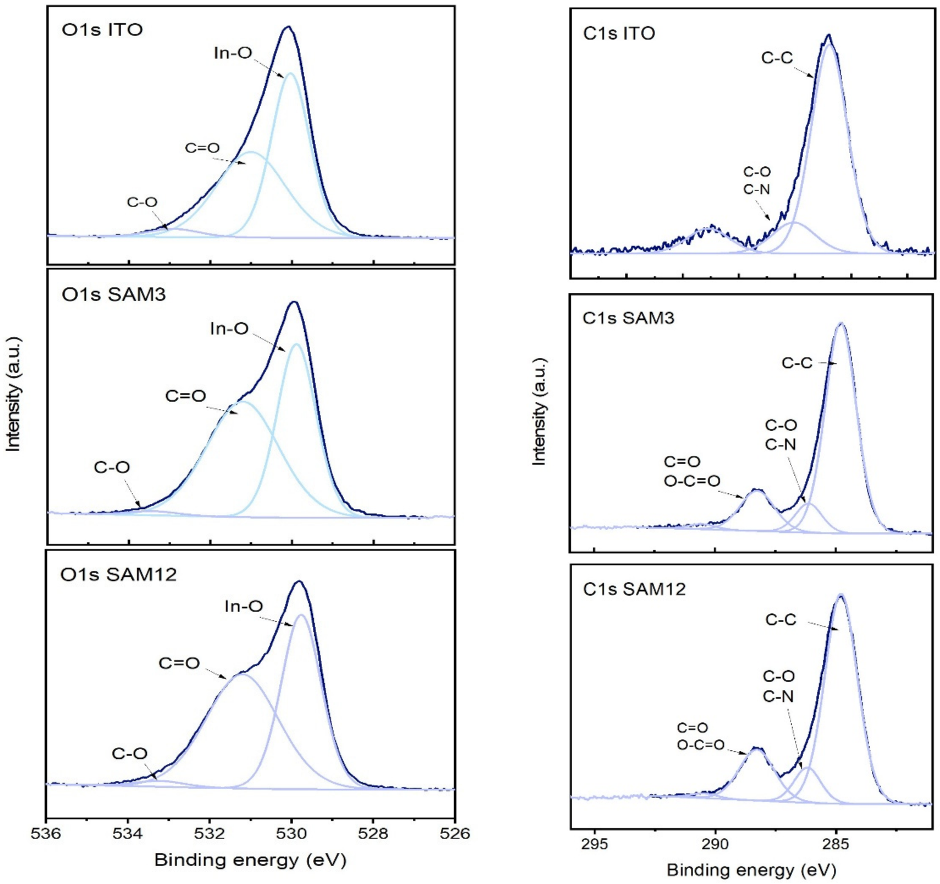

Figure S9. XPS high-resolution survey spectra of O1s and C1s on ITO, ITO/**SAM3** and ITO/**SAM12**.

Table S1. XPS elemental quantification from the XPS measurements of SAMs coated on ITO and bare ITO.

Sample	**Atomic concentration (%)**				
	In 3d	Sn 3d	C 1s	O 1s	N 1s
ITO/SAM3	23.24 ± 0.02	2.71 ± 0.01	37.35 ± 0.04	33.81± 0.04	2.88 ± 0.02
ITO/SAM12	24.02 ± 0.02	2.84 ± 0.01	33.25 ± 0.05	37.00± 0.04	2.88 ± 0.02
ITO	38.67 ± 0.03	4.43 ± 0.01	8.69 ± 0.04	48.22± 0.04	0

Sample	**Atomic concentration (%)**			
	C-O /C-N	C-C/C-H	C=O/O-C=O	π-π*
ITO/SAM3	8.78	74.05	15.63	1.53
ITO/SAM12	9.61	70.7	18.41	1.27

Table S2. PL lifetime decay of the ITO/ETL/QD films measured after excitation at 405 nm, recorded at 650 nm after acquisition of 5000 cps. The quality of the fitting is described by the χ^2 parameter.

Sample	**τ_1 (ns)**	**A_1 (%)**	**τ_2 (ns)**	**A_2 (%)**	**τ_{av} (ns)**	**χ^2**
ITO/QD	5.04±0.14	11.5	24.21±0.39	88.5	20.6	1.0
ITO/SAM3/QD	4.59±0.11	15.7	17.66±0.13	84.3	17.1	1.1
ITO/SAM12/QD	4.71±0.11	17.6	18.07±0.14	82.4	17.4	1.1

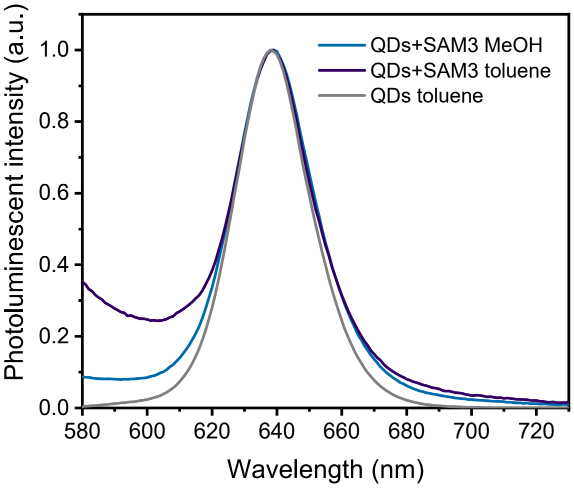

Figure S10. PL spectra of the solutions of QD in toluene and QD mixed with **SAM3** in toluene or in methanol after excitation at 450 nm.

Table S3. Optoelectronic characterization of the devices where **SAM3** and **SAM12** are tested as electron selective contacts in *n-i-p* configuration in LEDs.

Device	**Average Luminance values (cd/m^2)**	**Luminance of the champion device (cd/m^2)**
SAM3	1013 ± 161	1295
SAM12	1332 ± 52	1388
NO ETL	1381 ± 167	1628

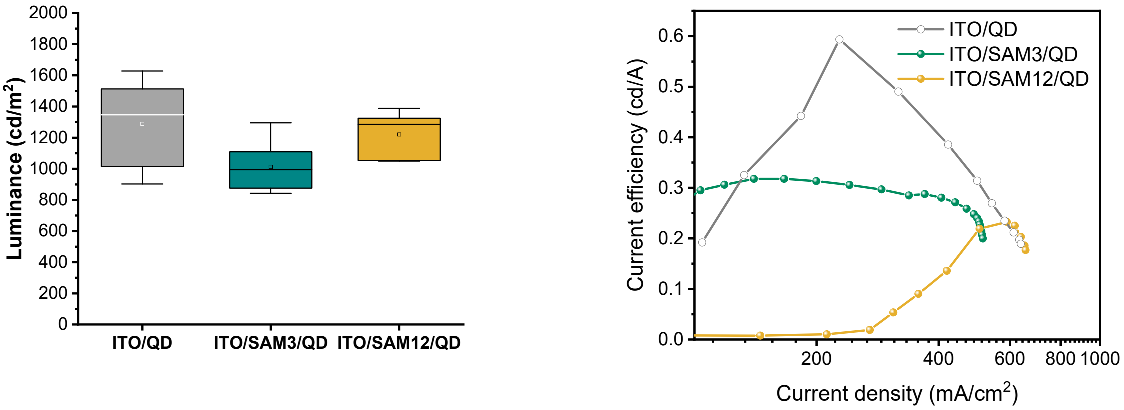

a **b**

Figure S11. (a) Luminance statistics for *n-i-p* devices, and (b) Variation of current efficiency with applied bias in *n-i-p* devices.

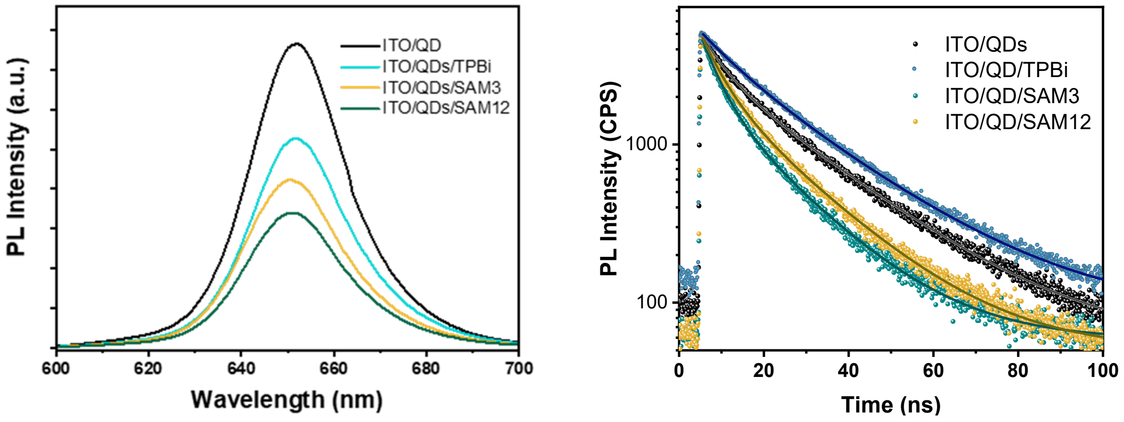

a **b**

Figure S12. PL emission spectra (a) and PL emission decays (b) of ITO/QDs and ITO/QDs/ETLs films after excitation at 405 nm and acquisition of 5000 cps at 650 nm. The continuous line represents the fitting of the decay to the biexponential Equation S2.

Table S4. PL lifetime decay of the ITO/QD/ETL films measured after excitation at 405 nm and acquisition at 650 nm for 5000 cps. The quality of the fitting is described by the χ^2 parameter.

Sample	τ_1 (ns)	A_1 (%)	τ_2 (ns)	A_2 (%)	τ_{av} (ns)	χ^2
ITO/QD	5.30±0.14	13.3	21.46±0.18	86.7	20.9	1.1
ITO/QD/TPBi	8.49±0.51	13.1	22.48±0.39	86.9	21.7	1.0
ITO/QD/SAM3	4.19±0.07	26.5	15.85±0.14	73.5	14.8	1.1
ITO/QD/SAM12	4.81±0.09	22.5	17.43±0.15	77.5	16.5	1.1

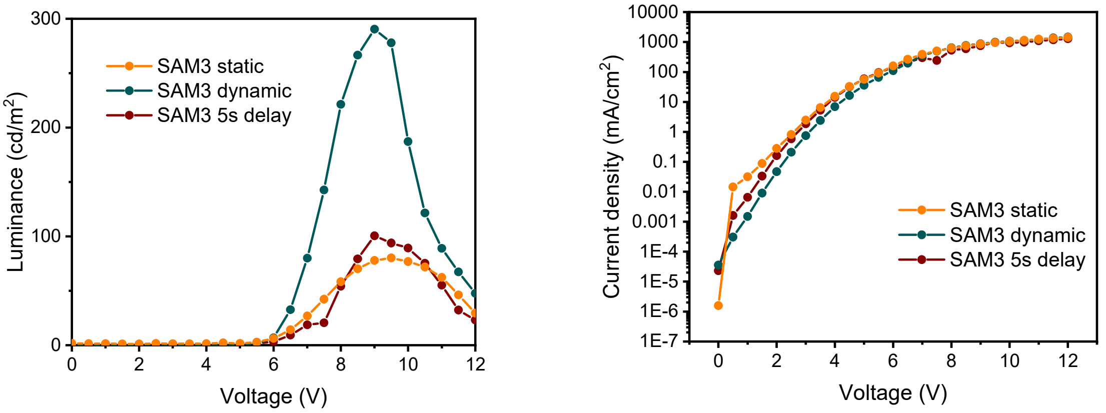

a **b**

Figure S13. Luminance (a) and current density dependence (b) with applied bias for *p-i-n* devices prepared with **SAM3** deposited under different conditions.

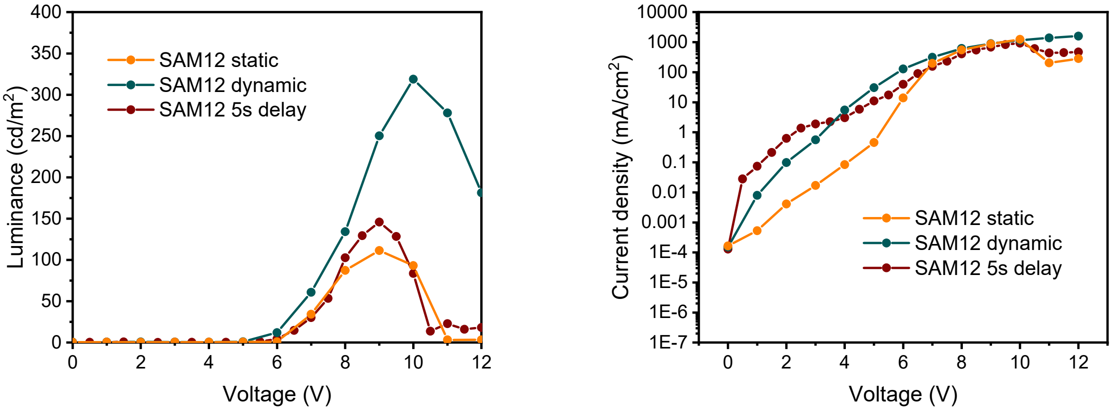

a **b**

Figure S14. Luminance (a) and current density dependence (b) with applied bias for *p-i-n* devices prepared with **SAM12** deposited under different conditions.

Table S5. Optoelectronic characterization of the *p-i-n* devices where **SAM3** and **SAM12** have been deposited in dynamic mode.

Device	Average Luminance values (cd/m^2)	Luminance of the champion device (cd/m^2)
SAM3	207 ± 48	249
SAM12	267 ± 67	367
TPBi	363 ± 74	450

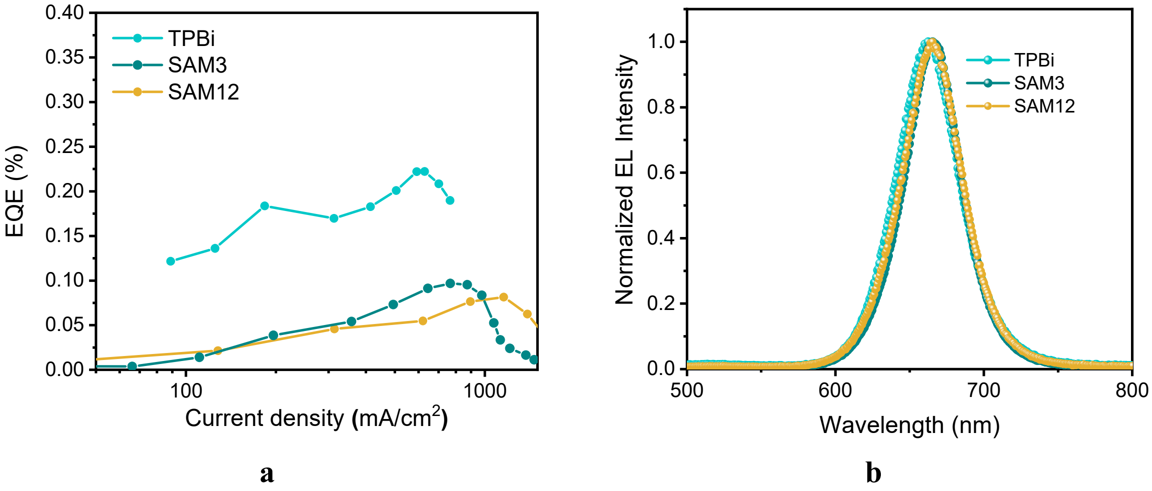

Figure S15. (a) EQE and (b) EL spectra for *p*-*i*-*n* devices.